Analysis of Generator Forced Oscillations During MOD 25 Testing Exploiting Wavelets

Chetan Mishra[1], Luigi Vanfretti[2], Mark Baldwin[1], Jaime Delaree Jr.[1], Kevin D. Jones[1]
[1]Dominion Energy, VA, US
chetan31@vt.edu, {mark.w.baldwin, j.de.la.ree, kevin.d.jones}@dominionenergy.com
[2]Rensselaer Polytechnic Institute, NY, US
luigi.vanfretti@gmail.com

Abstract

This paper presents a measurement-based analysis of a 1.5 Hz forced oscillation triggered during a reactive power capability test conducted at a power plant in Dominion Energy's power system. Owing to the slow evolving nature of the critical mode, it is demonstrated how time-frequency analysis of the period leading to the oscillation holds crucial information for finding the oscillation's source. Furthermore, it is shown how the use of wavelets enables to more granular analysis of the evolution and impact of the forced oscillation – a capability that will help Dominion better monitor and regulate the dynamic components of an evolving grid.

Keywords: Forced oscillations, time-frequency analysis, synchrophasor

1 Introduction

Dominion Energy has been investigating and developing data-driven processes to supplement the conventional model-based analysis of power system dynamics (Wang et al., 2022; Xu et al., 2023). Furthermore, in certain situations, it is used as a first resort due to the rising deployment of synchrophasor technology coupled with challenging modeling issues that remain unresolved. Today's power grid is experiencing an ever growing number of extraordinary oscillations that are triggered locally, including forced oscillations (Sarmadi & Venkatasubramanian, 2016). The appearance of different types of unwanted dynamics (Mishra et al., 2022; Wang et al., 2022) can be attributed in part to system integration design challenges, including the increasing reliance in black-box models that lead to suboptimal control design. This is becoming evident in the case of controllers for converter-based resources (Wang et al., 2022) that are typically installed in weak portions of the system (due to the low-cost of land) and a lack of incentives/requirements in controller and overall plant performance monitoring. Fortunately, when it comes to traditional synchronous machine-based power plants, their models are in general well understood and are systematically validated periodically (approximately every two years) as enforced by various standards (*PJM - Planning Modeling Submissions (MOD-026, 027 & 032)*, n.d.) so that they are accurately represented in different simulation software tools for engineering studies.

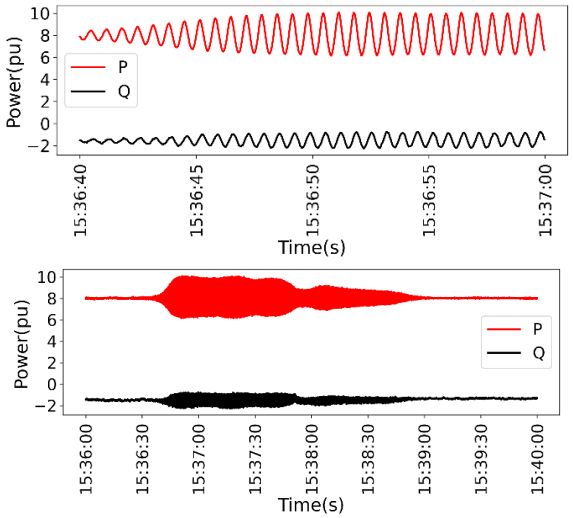

Figure 1. PMU Measurements of Real (P) and Reactive Power (Q) from Substation A (Test Plant, see Figure 2) Entire Test Window (bottom), Zoomed In (top).

One such standard is MOD 25-2 (*MOD-025-2*, n.d.), whose purpose is to ensure that accurate information on generator capability (gross net, real and reactive power) and synchronous condenser capability (reactive power) is available for planning models, which Dominion uses to assess Bulk Electric System (BES) reliability. The expected outcome of the test is the characterization of generator's capability

URI: https://hdl.handle.net/10125/106747
978-0-9981331-7-1

curves in the PQ plane, which include thermal limits as well as under and over excitation limiters on the excitation system. If during the test, the plant/unit fails to reach the expected output, an engineering analysis is to be performed to understand the root cause. The present work demonstrates how measurement data can provide an efficient means for such analysis and proves to be indispensable in certain scenarios. This case being investigated also shows that the use of highly accurate simulation models, such as that of a synchronous generator, does not necessarily lead to a well-controlled system. Furthermore, the use of conventional simulation models did not lead to accurate or relevant predictions of real-time behavior observed from measurement data, as presented in this paper. Our stance is that there is a great need for an alternate approach to assess power system operations thoroughly, and thus, going beyond conventional physics-based modeling and simulation studies is essential for the future of understanding and managing the grid. The measurement data analyzed here involved a region of the power system reaching small signal security limits before the plant could meet the expected output as shown in Figure 1.

It is important to highlight that the time-period before the test is just as significant as that during the test itself when studying this type of scenario. The pre-test behavior is characterized by small random perturbations with a slowly changing equilibrium and a stable linear response around it, referred to as ambient conditions (Pierre et al., 1997). Spectral analysis techniques (Stoica & Moses, 1997) have provided effective means to extract and analyze underlying dynamic processes independently and have proven to be effective in analyzing wide area oscillations in real world power systems (Hauer et al., 2007) (Kosterev, 2019; Pierre et al., 2012). On the other hand, during the test the system is marginally stable and therefore exposes different characteristics. Locating the source of undamped periodic motion (forced oscillation) is a challenging problem. particularly in situations with resonance between system modes and the forcing. In this regard, methods such as that of "energy flow" proposed in (Chen et al., 2013), could yield misleading results (Zhi & Venkatasubramanian, 2021) when the passivity condition w.r.t. the energy function formulation is violated. In non-resonance cases, which comprise most local oscillation events (such as the one being analyzed here), a simple approach using mode shapes of carefully chosen signals proves to be sufficient.

The contribution of this work is to propose an analysis methodology that can enable a human analyst to investigate similar real world forced oscillation cases beyond the quantification aspects (i.e., what is the oscillation frequency and its location). More importantly, it demonstrates how time-frequency analysis (using Wavelets) of the time-period leading to the oscillation can yield additional insights, which is a key contribution of our work. The remainder of this paper is organized as follows, Section 2 introduces the MOD-25 test location and its surroundings in Dominion Energy's system, Section 3 provides a background in signal processing techniques used in this work as well as a brief theoretical analysis of their application to ambient data from the test. The analysis results are presented in Section 4, followed discussion in Section 5.

2 Emergence of a Forced Oscillation During MOD-25 Testing

2.1 Study System

The focus of this analysis is a 500 kV region of Dominion's network, as shown in Figure 2. The green lines represent the 500 kV network, while 115 kV network is shown by red lines. The MOD 25 test was conducted on unit S of substation A, a power generation facility with three identical 435 MVA Combustion Turbine (CT) generator units (A, B, and C) and one 795 MVA steam unit, denoted as "S". A similar power generation facility is present at substation B, while substation C has a ±125 MVAR STATCOM, which are the two other important dynamic resources in the region. PMU measurements at 30 Hz are available at A, B, C and D for the time-period of interest, albeit with significant data dropouts.

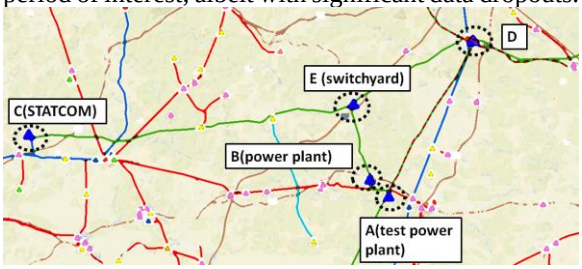

Figure 2. One Line Diagram, 500 kV (green), 115 kV (red).

2.2 Oscillation Event

Because each unit in substation A exceeds a 20 MVA rating, the MOD-25 standard required that the real power (P) and reactive power (Q) capability of each unit had to be assessed individually rather than as an aggregate. In accordance with this requirement, on August 2021, unit S was gradually brought to its minimum output of 320 MW, followed gradually reducing its voltage setpoint to operate at leading

power factor. The engineers performing the test brought it to a halt after about 3 minutes of observing sustained oscillations of about ±200 MW at the plant, starting from 15:36:38 UTC as shown in Figure 1. This forced oscillation does not propagate far from source and only interferes with local dynamics. An initial hypothesis drawn by the plant's test engineers was that this oscillation was due to the plant fighting against the nearby STATCOM at C, which is shown to be incorrect in the analysis presented in Section 4.

3 Spectral Analysis Background

Power system measurements from normal operation (ambient condition) can be approximated by a stochastic linear system. In this work, the time-period of analysis is separated depending on the system behavior. There are two major time-periods for our analysis, pre-event and during event. Pre-event is marked by a gradually changing voltage setpoint, and therefore a change in the plants' operating condition, eventually leading close to instability and thus, better represented by a time-varying linear system. Meanwhile, during the oscillation event, the system experiences a sustained oscillation and the signal's power is relatively stationary as the plant operator immediately halted the test on observing the oscillations. This separation in the analysis of time-periods allows us to choose the most appropriate signal processing tools to analyze them.

3.1 Power Spectral Density

Let the power spectral density (PSD) S(ω) (Stoica & Moses, 1997) of a stochastic signal x(t) be defined as its expected power distribution over frequency, i.e.,

$$\int S(\omega)d\omega = \lim_{T\to\infty}\frac{1}{T}\int_{-\frac{T}{2}}^{\frac{T}{2}} E(|x(t)|^2)dt \quad (1)$$

where $E(\,)$ is the expectation operator. Sustained oscillations at fixed frequencies will be distinguishable as Dirac delta terms. The system will be characterized by a time-invariant PSD and therefore, it is a good tool to characterize the underlying system dynamics from the available measurements. Now, in practice, because only a single measurement set from the plant's test is available, Welch's method (Stoica & Moses, 1997) is used. Welch's method realizes the expectation operator by dividing the data window into smaller blocks and averaging the PSD estimate across them. This sacrifices frequency resolution in exchange for an estimate with lower variance.

3.2 Time-Frequency Analysis using Wavelet Transform

The main challenge in applying the PSD for the entire pre-event testing time-period is that the system has a time-varying spectrum and therefore, a PSD estimate would not be able to gain much insight into the evolution of system, i.e., to characterize the oscillation mode going from stable to critically stable. Consequently, time-frequency analysis techniques (a class of linear techniques) that aim to track the time-varying spectrum (Priestley, 1988) are more appropriate. These techniques take the inner product of the signal with a family of pre-assigned signal templates skewed in both time and frequency. However, there is a trade-off between time and frequency resolutions. The Continuous Wavelet Transform (CWT) (Daubechies, 1990), which is employed in the present work, can provides a good trade-off favoring frequency resolution. This is achieved by assuming that low frequency dynamics change less rapidly than high frequency ones and therefore increasingly favoring frequency resolution over time resolution at lower frequencies. Starting with a function called the mother wavelet $\psi(t)$, templates denoted by $\psi_{a,b}(t)$ are created using translation and dilation operators on it as follows: $\psi_{a,b}(t) = a^{-\frac{1}{2}}\psi((t-b)/a)$. Here, a (scale factor) has the effect of stretching $\psi(t)$ (shift towards lower frequencies) while b (shift factor) introduces a phase shift, i.e., translating in time. Finally, the corresponding wavelet coefficient $W(a,b)$ for a signal $x(t)$ is obtained as,

$$W_x(a,b) = \int x(t)\bar{\psi}_{a,b}(t)dt \quad (2)$$

where, $\overline{(\,)}$ is the complex conjugate operator. The mother wavelet, $\psi(t)$, is designed to have a compact time and frequency support, i.e., translating and scaling it is comparable to a band pass filter paired on the windowed original signal. In the present work, we use the Morlet wavelet, which consists of complex sinusoid modulated with a Gaussian $\psi(t) = e\text{^}(-\frac{(2\pi^2t^2)}{k_0^2}) \times (e^{j2\pi t} - e^{-\frac{k_0^2}{2}})$, where the envelop factor k_0, which is set to 6, controls the number of oscillations in the wave packet, i.e., frequency dependent window width.

3.3 Application to Pre-Event Ambient Data

Next, it is important to understand the information contained in the CWT coefficients when applied to the pre-event time-period leading to the oscillation. The measurements from this time-period can be modeled

as outputs from a time-varying linear system driven by stationary Gaussian white noise input $u(t) \sim N(0,1)$ as,

$$x(t) = \int h(t,\tau)u(t-\tau)d\tau = \int e^{j\omega t}H(t,\omega)dz(\omega) \quad (3)$$

where $h(t,\tau)$ is the time-varying impulse response representing the effect of input at time $t-\tau$ on the output at time t, $H(t,\omega) = \int h(t,\tau)e^{-j\omega\tau}d\tau$, defining the time-varying power spectral density of $x(t)$ as $|H(t,\omega)|^2$ and $z(\omega)$ being a 0 mean stochastic process with orthogonal increments, i.e., $E(dz(\omega)) = 0, E(dz(\omega)dz^*(\omega_1)) = \delta(\omega-\omega_1)d\omega$. Here, the peaks of the time-varying spectrum will correspond to the evolving modes of the underlying power system. The wavelet coefficients for this system are,

$$W_x(a,b) = \iint e^{j\omega t}H(t,\omega)\bar{\psi}_{a,b}(t)dtdz(\omega). \quad (4)$$

Assume that the time support of the mother wavelet $\psi(t)$ is $\pm\Delta T$ s, while its frequency support is $\omega_0 \pm \Delta\omega\ rad/s$. Consequently, for $\psi_{a,b}(t)$, these are $\omega\_0/a \pm \frac{\Delta\omega}{a}$ and $b \pm a\Delta T$, respectively. Let the critical mode's (the one becoming unstable) fundamental frequency be denoted as $\omega_{crit}(t)$ during the time-period of analysis and assume that it largely overlaps with the frequency band corresponding to the scale parameter value a^*. Since the setpoint is changed slowly during the test, the signal in that frequency band (representing both the critical mode and other dynamics) can be assumed to be quasi stationary, i.e., $H(t,\omega) \approx H(b,\omega)\forall(\omega,t) \in (\frac{\omega_0}{a^*} \pm \frac{\Delta\omega}{a^*}, b \pm a^*\Delta T)\forall b$, transforming Eq. (4) to

$$W_x(a^*,b) \approx \int H(b,\omega)\overline{\left(\hat{\psi}_{a^*,b}(\omega)\right)}dz(\omega)$$
$$E(|W_x(a^*,b)|^2) \approx \int |H(b,\omega)|^2\left|\hat{\psi}_{a^*,b}(\omega)\right|^2 d\omega \quad (5)$$

where $\hat{(\ )}$ is the Fourier transform. Thus, $E(|W_x(a,b)|\text{^}2)$ at $a = a^*$ represents a weighted sum of the underlying signal spectrum in the corresponding time window $|H(b,\omega)|^2$ with the weights given by spectrum of the corresponding wavelet. Now, as the critical mode approaches zero damping and consequently becoming marginally stable, the integral in Equation (5) will be dominated by the term $\left|H\left(b,\omega_{crit}(b)\right)\right|^2|\hat{\psi}_{a^*,b}(\omega_{crit}(b))|\text{^}2$, i.e., a scaled spectrum of critical mode dynamics (Brincker et al., 2001). Thus, scalogram coefficients are sufficient for tracking the evolution of that mode towards instability.

4 Analysis

4.1 Wide Area Voltage Analysis

First, it is necessary to understand the fundamental frequency of the triggered oscillations. This is achieved by plotting the PSD estimates for the voltage magnitude measurements of substation A for the pre-testing time-period and during event window, which are contrasted in Figure 3. As it can be seen, there was only one faintly observable mode at approximately 5 Hz prior to the test, however, when the test is carried out, a 1.5 Hz high energy component is introduced together with its harmonics at 3 and 4.5 Hz, and the original 5 Hz component vanishes. As a result, the 1.5 Hz frequency is unlikely to resonate with the system, and a simple mode shape analysis would be sufficient to identify the source.

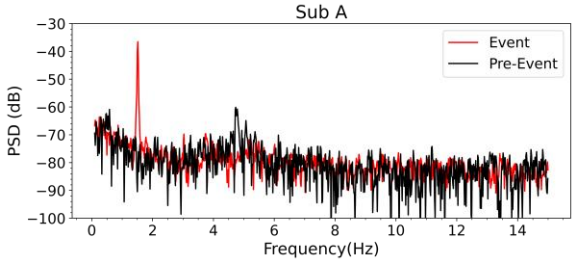

Figure 3. Voltage Magnitude PSD Pre-Event (black), Event (red).

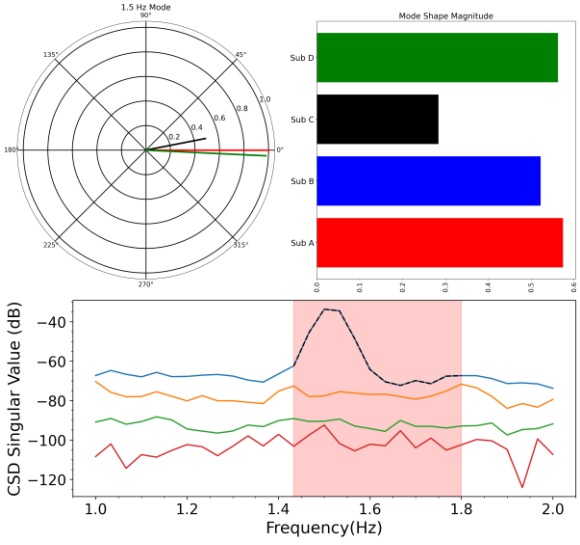

Figure 4. Voltage Magnitude Mode Shape (top), CSD Singular Values (bottom).

Next, using frequency domain decomposition (FDD) (Brincker et al., 2001), the 1.5 Hz mode shape is estimated from the 500 kV voltage magnitude measurements to pinpoint the oscillation's source, as shown in Figure 4. According to the estimated mode shape, substation A's 500 kV voltage magnitude has a higher participation in the oscillation than the other substations nearby. Additionally, substation C oscillates almost in phase with others while having a much smaller contribution to the oscillation. This shows that the STATCOM at substation C is effectively controlling its terminal voltage, which results in suppressed oscillations, and that it is not actually oscillating against the test units at substation A, which nullifies the hypothesis of the plant operators. FDD also provides information about the presence of multiple modes at the same frequency, given by the singular values of the cross spectral density matrix as plotted in the bottom plot in Figure 4. As the figure show, there is only one significant peak at 1.5 Hz, indicating that only one mode is being observed.

4.2 Analysis of Line Flows for Source Localization

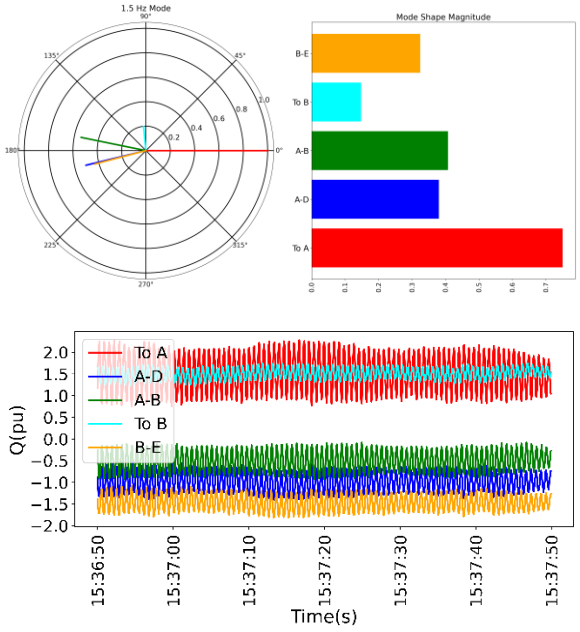

Figure 5. Q Flow 1.5 Hz Mode Shape (top) and Q Flow Measurements (bottom).

The fact that the voltage magnitude measurements at the 500 kV level are tightly coupled and coherent makes it incredibly challenging to identify the source(s) of the oscillations. On the other hand, MVA flows can be quite helpful in this analysis owing to the power balance constraints from KCL. Here we adopt a systems approach (Chompoobutrgool & Vanfretti, 2013), which can be summarized as follows. In general, if the oscillation is local with no resonance, the source's P/Q output should have the highest participation in the oscillation with other control devices acting as a sink, contributing with smaller, out of phase inputs to the network to suppress the oscillation in voltage/angle. The 1.5 Hz mode shape obtained from Q flows is shown in the top plot in Figure 5. It shows that the Q oscillation amplitude that emerges from A is significantly larger than all the other individual 1.5 Hz Q flow mode shapes, which points towards A being the likely source. Additionally, it equally separates into two components that move towards the nearby generator B and substation D. This is unexpected because B is electrically closer to A and has an AVR within the generator, which should have been the main sink for this oscillation, but this was not the case. A close examination of the Q output of B (see bottom plot in Figure 5), reveals that this nearby power plant has a negligible contribution to the voltage regulation/control of this oscillation or its effects. Therefore, this power plant is circumvented, and the oscillation propagates to the other parts of the network.

4.3 Finding the Culprit Unit inside Substation A

Figure 1 shows that the final triggered oscillations involve a mode becoming unstable with the system trajectory settling on a limit cycle (observed as oscillations during the event). With sufficient data to support the claim that the oscillation originates from A: is it possible to understand the nature of the instability solely through measurements?

Answering this question requires a measurement time-period during which the critical mode is stable and observable to gain a sense of the participation of the various generator units inside plant A. This is because once an oscillation becomes critically stable, the resulting measurements represent the system's large signal/nonlinear response, where the actual modal properties may be lost. As seen previously in Figure 3, the pre-event spectrum did not have a spectral peak in the modal frequency range of 1.5 Hz. However, this only means that a majority of and not the entirety of the pre-event time window used for estimating the spectrum had an unobservable critical mode, which was lost with the averaging applied by Welch's method. Thus, an estimate of the time-varying spectrum is obtained first through a wavelet scalogram, as shown in Figure 6. This was obtained from plant A's net PQ output during the 1-minute time-period leading to the event. Note that the CWT

scalogram plot's frequency axis is set to the central frequency relevant for each scale.

Analyzing Figure 6 would suggest that the nature of instability is angular in nature because the mode appears earlier in P than in Q. This is improbable, though, owing to the critical mode's frequency being too high for electromechanical mode of a plant as large as this (Rogers, 1996). Additionally, please note that the plant's net PQ output on the high side (500 kV) is plotted, which may not be the best observer for these dynamics at the generator level (Brincker et al., 2001). Therefore, it is necessary to contrast these results to those obtained from voltage magnitude measurements of the generator units in substation A, as shown in Figure 7. Recall that at substation A, there are three identical 435 MVA CT generator units (A, B, and C) and one 795 MVA steam unit, S.

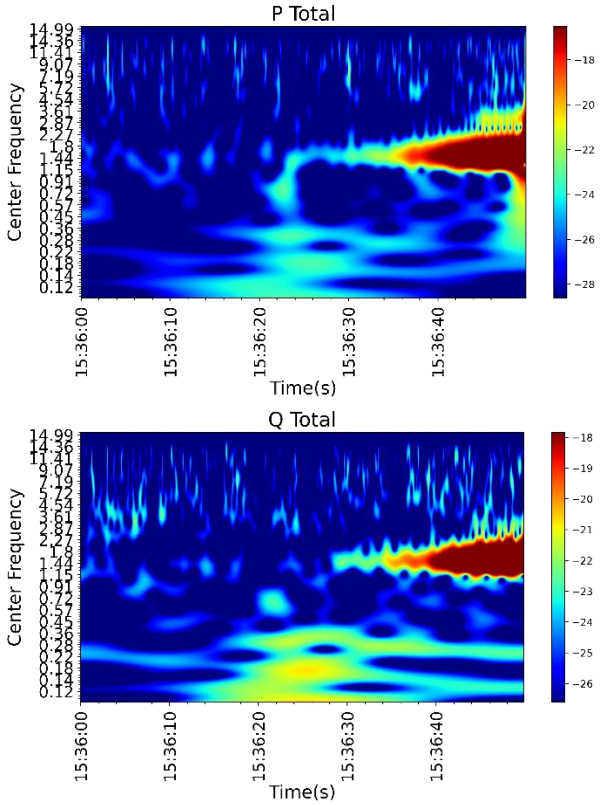

Figure 6. Plant A Net Output Scalogram.

Because units A, B and C are similar, only unit A is analyzed. The oscillation in the terminal voltage is observed only at unit S before it becomes unstable and is consequently large enough to impact all the other units. This reduced observability could be due to the unit step up transformers playing the role of filters and/or the response of the AVRs at the other units (A, B and C). However, for this to happen, the Q outputs of those units would need to respond (and therefore observe the mode), which is not the case as shown in Figure 8. In addition, observe in Figure 8 that the MW oscillations at unit S start precisely at the same time as V (and Q) oscillations. *Therefore, keeping the oscillation frequency in mind, it is certain that the mode is a result of the local AVR response of unit S. Consequently, the P oscillations at unit S are triggered due to P-V dynamic coupling.*

The last phenomena to comprehend is the nature of the limit cycle that unit S enters after the system becomes unstable, which is difficult to confirm without the help of simulation models. However, based on our experience, limit cycles resulting from unstable voltage controllers interacting with limiters (Reddy & Hiskens, 2005) are far more common than super critical Hopf bifurcation in real-world power systems.

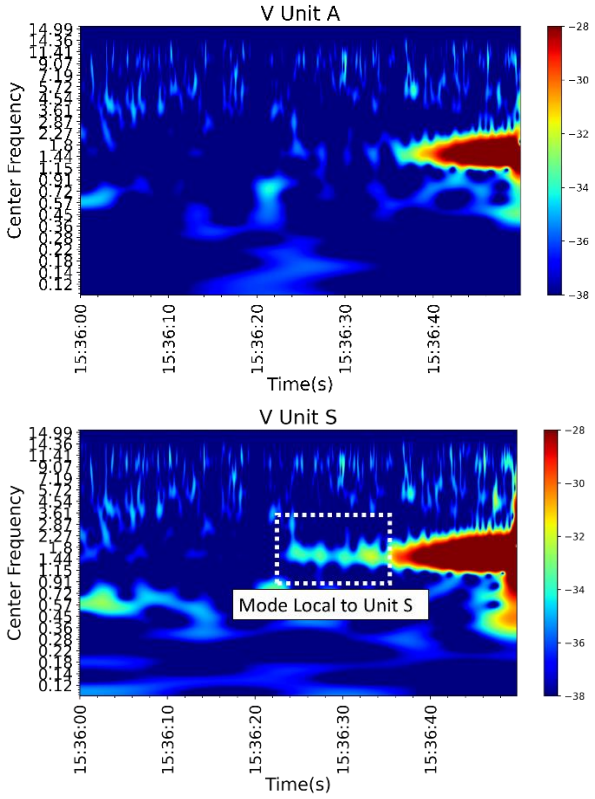

Figure 7. Generator Terminal Voltage Scalograms.

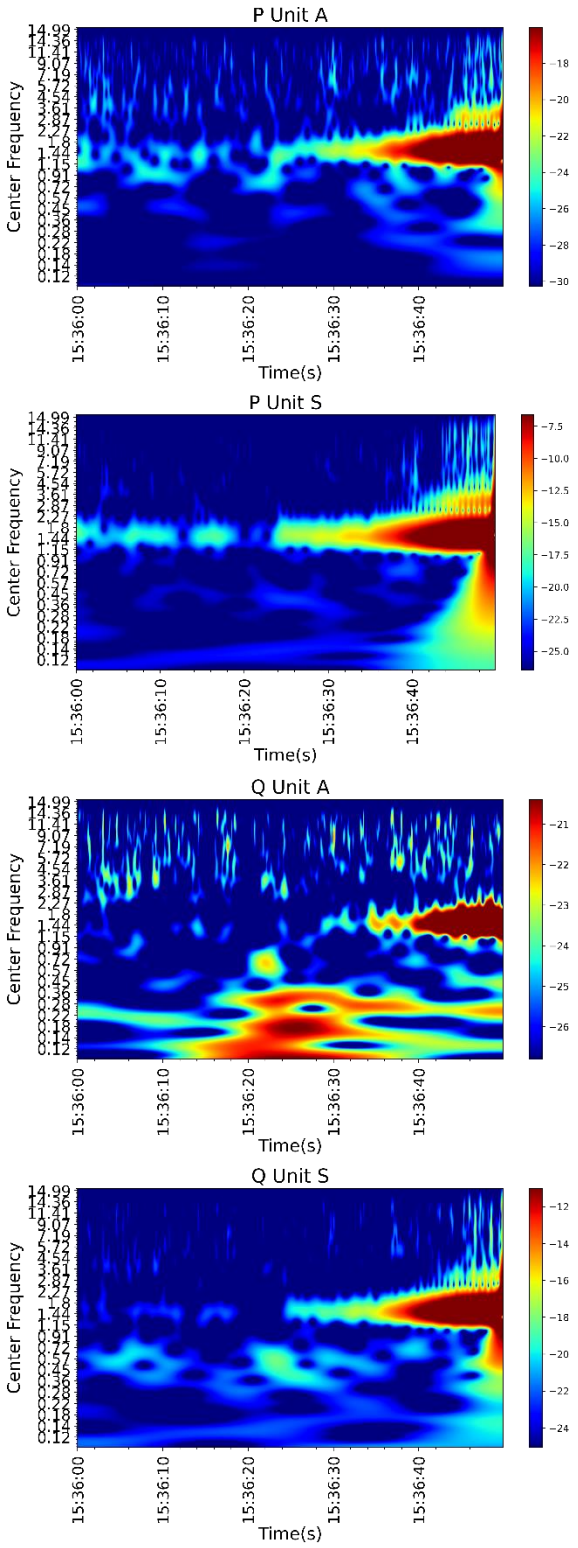

Figure 8. PQ Output of Units in Substation A.

4.4 Retuning Culprit Unit and Subsequent Process Changes

One of the key conclusions of this investigation was that the culprit unit's power system stabilizer was not tuned to cover light load points in the generator's leading region. Indeed, the common industry practice has been to tune and test stabilizers only at full load lagging conditions. Dominion had the stabilizer subsequently retuned to cover this previously neglected, but critical, load region. As a result, Dominion determined that all future tuning and testing work for excitation systems must be conducted also under light loading. Consequently, the tuning process now covers a more complete region of the generator's allowable operating points. The result has led to a more comprehensive tuning and validation process, thus improving local and zone-wide stability. The findings also have more far-reaching benefits as the consulting firm that tuned the stabilizer is preparing a proposal to include these new requirements in NERC's excitation system validation standard.

5 Conclusions and Future Work

This work presents an analysis of a forced oscillation using synchrophasor data that emerged during a reactive power capability test at a power plant in Dominion Energy's system. The proposed approach uses time-frequency analysis techniques to extract the otherwise overlooked information in the time-period prior to the oscillation, which is critical to pinpoint the source down to the unit level as well as nature of the instability resulting in the final oscillation. Future work will aim to verify the emergence of the mode because of the test generator reaching its AVR limits and entering a limit cycle during the test.

6 References

Brincker, R., Zhang, L., & Andersen, P. (2001). Modal identification of output-only systems using frequency domain decomposition. Smart Materials and Structures, 10(3), 441. https://doi.org/10.1088/0964-1726/10/3/303

Chen, L., Min, Y., & Hu, W. (2013). An energy-based method for location of power system oscillation source. IEEE Transactions on Power Systems, 28(2), 828–836. https://doi.org/10.1109/TPWRS.2012.2211627

Chompoobutrgool, Y., & Vanfretti, L. (2013). Identification of Power System Dominant Inter-Area Oscillation Paths. IEEE Transactions on Power Systems, 28(3), 2798–2807. https://doi.org/10.1109/TPWRS.2012.2227840

Daubechies, I. (1990). The wavelet transform, time-frequency localization and signal analysis. IEEE Transactions on Information Theory, 36(5), 961–1005. https://doi.org/10.1109/18.57199

Hauer, J. F., Trudnowski, D. J., & DeSteese, J. G. (2007). A Perspective on WAMS Analysis Tools for Tracking of Oscillatory Dynamics. 2007 IEEE Power Engineering Society General Meeting, 1–10. https://doi.org/10.1109/PES.2007.386186

Kosterev, D. (2019). Synchrophasor Technology at BPA. In S. (NDR) Nuthalapati (Ed.), Power System Grid Operation Using Synchrophasor Technology (pp. 77–127). Springer International Publishing. https://doi.org/10.1007/978-3-319-89378-5_4

Mishra, C., Yang, D., Wang, C., Xu, X., Jones, K. D., Matthew Gardner, R., & Vanfretti, L. (2022). Analysis of STATCOM Oscillations using Ambient Synchrophasor Data in Dominion Energy. 2022 IEEE Power & Energy Society Innovative Smart Grid Technologies Conference (ISGT), 1–5. https://doi.org/10.1109/ISGT50606.2022.9817489

MOD-025-2. (n.d.). Retrieved November 13, 2022, from https://www.nerc.com/pa/Stand/Pages/MOD0252RL.aspx

Pierre, J. W., Trudnowski, D., Donnelly, M., Zhou, N., Tuffner, F. K., & Dosiek, L. (2012). Overview of System Identification for Power Systems from Measured Responses. IFAC Proceedings Volumes, 45(16), 989–1000. https://doi.org/10.3182/20120711-3-BE-2027.00412

Pierre, J. W., Trudnowski, D. J., & Donnelly, M. K. (1997). Initial results in electromechanical mode identification from ambient data. IEEE Transactions on Power Systems, 12(3), 1245–1251. https://doi.org/10.1109/59.630467

PJM - Planning Modeling Submissions (MOD-026, 027 & 032). (n.d.). Retrieved November 15, 2022, from https://www.pjm.com/planning/services-requests/planning-modeling-submissions

Priestley, M. B. (1988). Non-linear and non-stationary time series analysis. London: Academic Press.

Reddy, P. B., & Hiskens, I. A. (2005). Limit-induced stable limit cycles in power systems. 2005 IEEE Russia Power Tech, 1–5. https://doi.org/10.1109/PTC.2005.4524706

Rogers, G. (1996). Demystifying power system oscillations. IEEE Computer Applications in Power, 9(3), 30–35. https://doi.org/10.1109/67.526851

Sarmadi, S. A. N., & Venkatasubramanian, V. (2016). Inter-Area Resonance in Power Systems From Forced Oscillations. IEEE Transactions on Power Systems, 31(1), 378–386. https://doi.org/10.1109/TPWRS.2015.2400133

Stoica, P., & Moses, R. (1997). Introduction to Spectral Analysis (1st edition). Prentice Hall.

Wang, C., Mishra, C., Jones, K. D., Gardner, R. M., & Vanfretti, L. (2022). Identifying Oscillations Injected by Inverter-Based Solar Energy Sources. 2022 IEEE Power & Energy Society General Meeting (PESGM), 1–5. https://doi.org/10.1109/PESGM48719.2022.9916830

Xu, X., Mishra, C., Wang, C., Jones, K., Starling, J., Gardner, R., & Vanfretti, L. (2023, April 10). Tracking Periodic Voltage Sags via Synchrophasor Data in a Geographically Bounded Service Territory. 2023 IEEE PES Grid Edge Technologies. 2023 IEEE PES Grid Edge Technologies, San Diego.

Zhi, Y., & Venkatasubramanian, V. (2021). Analysis of Energy Flow Method for Oscillation Source Location. IEEE Transactions on Power Systems, 36(2), 1338–1349. https://doi.org/10.1109/TPWRS.2020.3024866